

L. Costa, A.S.
Miranda, J.C.P. Claro
Universidade do
Minho, Departamento
de Engenharia
Mecânica, Guimarães,
Portugal, and M. Fillon
Solid Mechanics
Laboratory, University
of Poitiers, URM CNRS
6610, Futuroscope,
France

Temperature, Flow, and Eccentricity Measurements in a Journal Bearing with a Single Axial Groove at 90° to the Load Line

Abstract

Parametric experiments were conducted to analyse the influence of some supply conditions on the performance of a steadily loaded journal bearing. The temperature distribution on the internal surface, the flow rate, and the bearing eccentricity were measured for different sets of operating conditions, under variable supply conditions. Quantitative information was provided which showed the effect of both shaft speed and applied load on maximum bush temperature and flow rate. It was observed that flow rate was moderately affected by load and significantly affected by rotational speed, oil supply temperature, and supply pressure. The maximum bush temperature was moderately affected by supply pressure and load, and significantly affected by shaft speed. For low applied loads, the attitude angle was markedly affected by supply pressure. The experimental results also showed that for a small groove length there was a variation in bush temperature in the axial direction in the groove region.

Keywords

journal bearing, bearing performance, eccentricity, temperature distribution, flow rate, single axial groove

INTRODUCTION

Hydrodynamic journal bearings are currently designed to operate at high specific loads and high rotational speeds with good performance. Under these operating conditions, a significant amount of heat is generated by viscous shearing in the oil, raising its temperature. Furthermore, the supply conditions (supply pressure, supply temperature, and groove dimensions and location) dictate the flow rate, thereby affecting the oil temperature inside the bearing. As a result, the oil viscosity

Table 1 Essential bearing dimensions and oil viscosity characteristics

	Bearing		
	A	B	C
Bearing nominal diameter, d ($\times 10^{-3}$ m)	50	50	50
Bearing length, b ($\times 10^{-3}$ m)	40	40	25
Bush outer diameter, D ($\times 10^{-3}$ m)	100	100	100
Radial clearance at 23°C, C_r ($\times 10^{-6}$ m)	38.50	40.75	45.76
Length of supply groove, a ($\times 10^{-3}$ m)	20	32	20
Width of supply groove, w ($\times 10^{-3}$ m)	10	10	10
Groove location, ϕ (degrees)	90	90	90
Oil viscosity at 30°C, μ_{30} (Pa s)	0.0467	0.0467	0.0467
Oil viscosity at 75°C, μ_{75} (Pa s)	0.0083	0.0083	0.0083

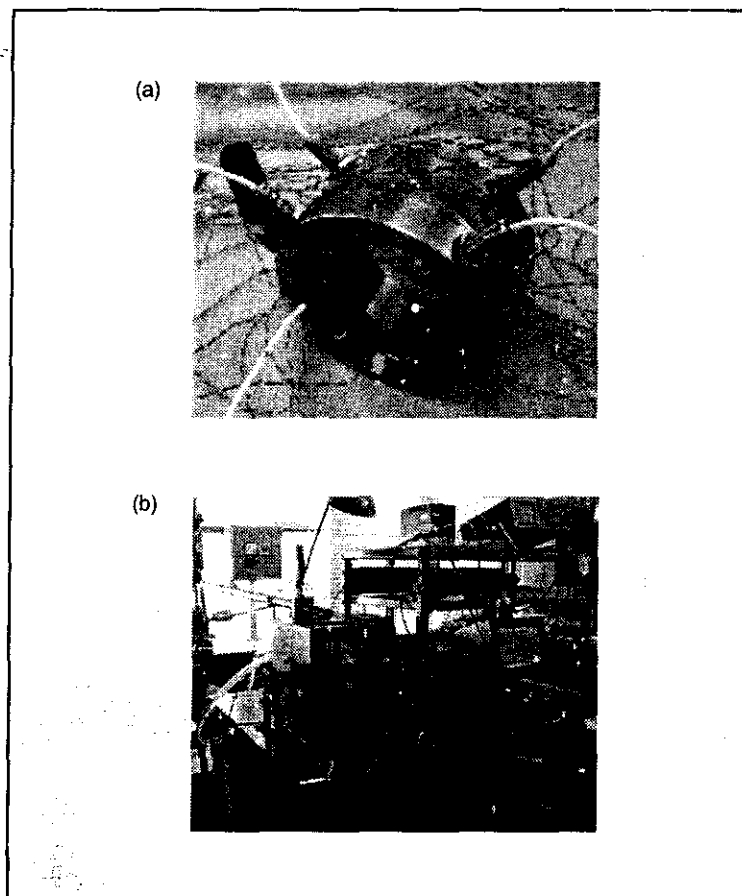
and bearing load capacity will be affected. Thermal effects in hydrodynamic lubrication therefore play a crucial role in the prediction of bearing characteristics. It is important for bearing designers to be able to predict to what extent the bearing performance will be affected by oil supply conditions.

In hydrodynamic journal bearings working in a steady-state regime, oil is usually supplied to the bearing through axial grooves. Very often in practical applications the bush cannot be installed with the lubricant supply groove on the load line. Alternatively, the bush can be mounted with the groove at 90° to the load line.

Experimental investigations of the thermohydrodynamic performance of journal bearings have been carried out over many decades,^{1,2} but there is little experimental information concerning the influence of the supply conditions on the thermal behaviour of journal bearings with one axial groove at 90° to the load line.³ Recent experimental investigations have been carried out using bushes with one groove on the load line,^{4,5} and two diametrically opposed axial grooves.^{6,7} According to published results, the supply conditions affect the bearing performance (maximum temperature, flow rate, power loss and friction torque) in different ways, making evident the need to

L. Costa, A.S. Miranda, J.C.P. Claro, and M. Fillon: Temperature, flow, and eccentricity measurements in a journal bearing with a single axial groove at 90° to the load line

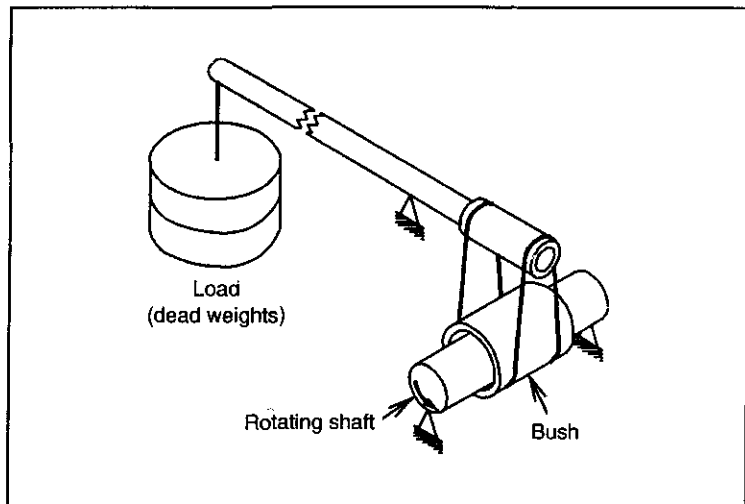
Figure 1 Photographs showing (a) the instrumented test bush and (b) a general view of the experimental apparatus



consider all supply parameters to give a more precise analysis of bearing performance. Some authors^{8,9} have encouraged experimental work in the field of thermal analysis in bearings, in order to enable the improvement of theoretical models.

This work aims to elucidate the effect of lubricant supply conditions on bearing performance and to add results to the stock of thermohydrodynamic data currently available for journal bearings. Three journal bearings with a single axial groove located at 90° to the load line were tested under steady load, laminar flow, for a range of variation of supply conditions, with different combinations of speed and load.

Figure 2 Test bearing loading system



BEARING GEOMETRY AND OIL SPECIFICATIONS

The characteristics at 23°C of the test bearings and lubricating oil used in the present work are given in **Table 1**. A photograph of one of the instrumented bushes, mounted in its cylindrical housing, is shown in **Figure 1(a)**. Bushes and housings were made of RG5G-CuSn5ZnPb bronze. A 35 mm thick bronze cylinder (bush) was pressed into a 15 mm thick bronze cylinder (housing). The bush inner diameter was measured using a high-precision analogue comparator with a resolution of 10^{-6} m. The rotating shaft (stainless steel X22-CrNi17) was ground to an ISO-N4 finishing quality. A high-precision coordinate measuring machine with a resolution of 10^{-7} m was used to measure the shaft diameter. The values of the bush inner diameter and shaft diameter were taken as the average of six measurements. The lubricant used was a mineral oil (Galp Hydrolep 32, ISO VG 32). The oil viscosity was obtained using a falling ball viscometer following the procedures specified by DIN 53097.

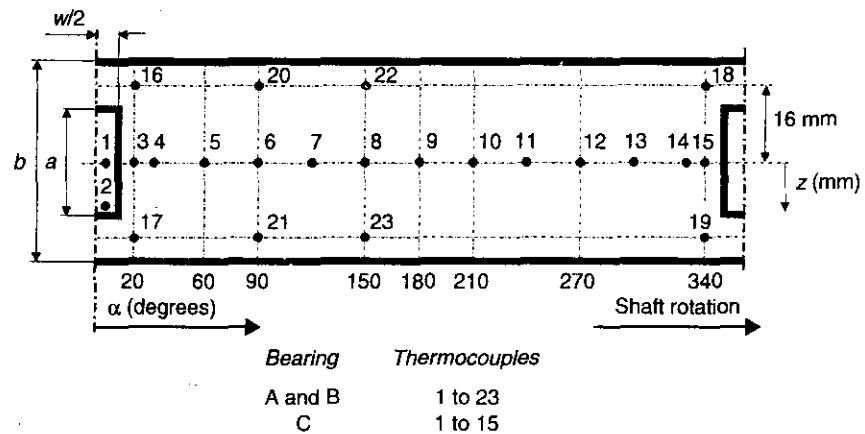
TEST RIG AND EXPERIMENTAL MEASUREMENTS

A test rig, which was initially designed and manufactured to investigate the influence of supply conditions on oil flow rate, was modified for the present work. Full details of the test rig can be found elsewhere.¹⁰ A brief description is given here.

A general view of the experimental apparatus is shown in **Figure 1(b)**. It basically consists of a test bearing, a

L. Costa, A.S. Miranda, J.C.P. Claro, and M. Fillon: Temperature, flow, and eccentricity measurements in a journal bearing with a single axial groove at 90° to the load line

Figure 3 Location of thermocouples (•) for temperature measurements



rotating shaft, a lubricant feeding system, a loading system, a temperature measurement system, and a digital oscilloscope connected to the displacement transducers used to measure film thickness.

The rotating shaft is rigidly mounted on to two high-precision conical roller bearings that are pre-loaded in order to remove any radial clearance and to ensure good stiffness. The shaft is driven through a timing belt by a continuously variable speed electric motor (0.95 kW). The rotational speed was measured with a reflection-type tachometer, which ensured a speed control to an accuracy of ± 2 rpm.

The loading system (Figure 2) consists of dead weights applied to a loading arm, acting through needle bearings on a closed-loop steel wire attached to the bush. The bearing applied load corresponding to a given set of dead weights was measured using a high-precision load cell with an error of less than ± 0.5 N.

The hydraulic pump (3.6×10^4 l/min, 16×10^2 kPa) was used to supply oil to the bearing. The flow rate was measured by a precision gear flow meter, which was calibrated for the range of operating oil viscosity, with an accuracy of $\pm 3\%$. Using a manual pressure-limiting valve and a pressure dumper, the oil could be supplied to the bearing at any pressure less than

Table 2 Basic test conditions

Parameter	Specifications
Speed, N (rpm)	2000, 3000, and 4000
Load, W (kN)	0.5, 1, 2, 3, and 4
Oil supply pressure, P_s (kPa)	100 and 300
Oil supply temperature, T_s (°C)	35 and 45
Ambient temperature, T_a (°C)	20 to 32

400 kPa. A pressure transducer located at the internal surface of the supply groove was used to measure the oil supply pressure with an accuracy of ± 0.8 kPa over the operating supply pressure range.

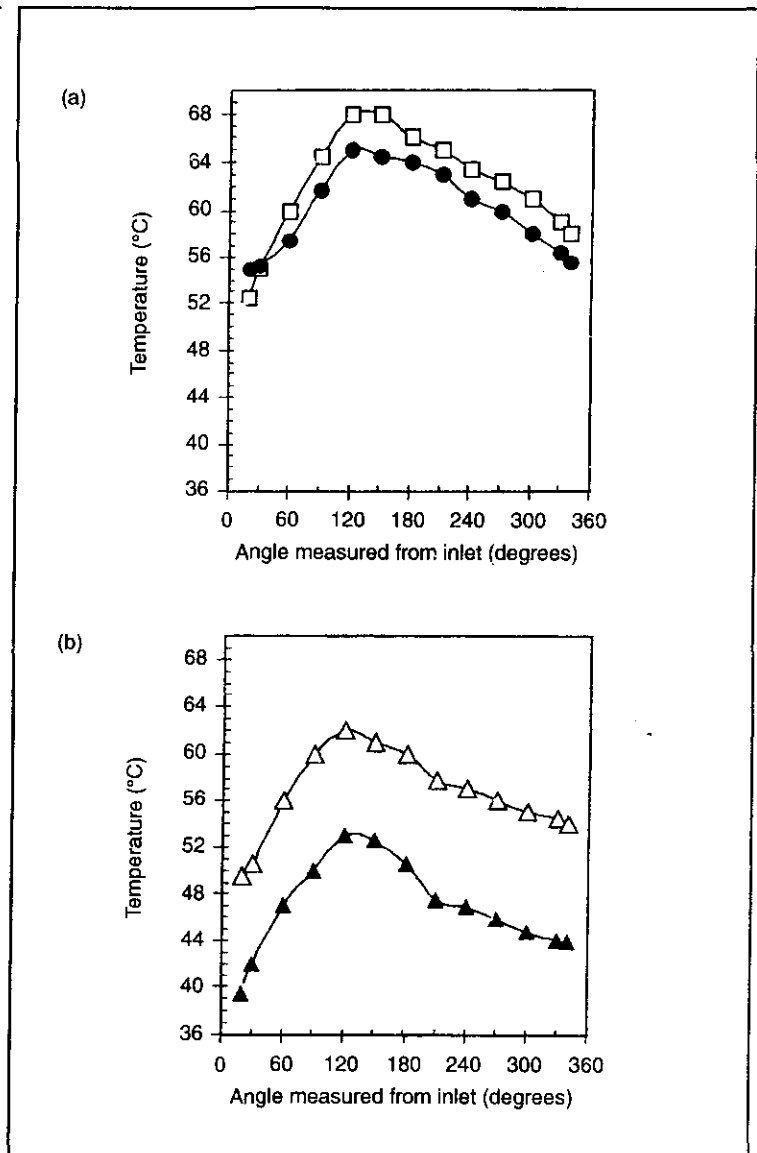
For temperature measurements type J thermocouples were mounted flush with the internal surface of the bush. Twenty-one thermocouples were used in bearings A and B, while 13 thermocouples were used in bearing C. The circumferential and axial locations of the thermocouples are shown in **Figure 3**. In order to measure the oil supply temperature two thermocouples were used in the flexible feeding tube at the bearing entry. Additional thermocouples were mounted in order to measure the oil groove temperature, the environment temperature, oil drain temperature, and oil tank temperature. The signals provided by the thermocouples were monitored using a data acquisition card of a computer. Each thermocouple was calibrated by comparing its reading of water temperature in a thermostatic vessel with that of a high-precision analogue thermometer. The discrepancies observed were within the range $\pm 1.25^\circ\text{C}$, this being assumed to be the accuracy of the thermocouples.

The bearing eccentricity ratio and attitude angle were calculated from measurements of film thickness using four displacement transducers situated in transverse planes set in the front and back of the bearing. Signals from these transducers were transferred to a digital oscilloscope, the indicated displacement being used to determine the bush position in relation to the shaft centre. For this purpose it was necessary to estimate the shaft and bush thermal expansion, considering

Figure 4 Circumferential temperature profiles at the inner surface of the bush on bearing mid-plane for different operating conditions:
 (a) bearings A and B
 $W = 4 \text{ kN}$
 $N = 4000 \text{ rpm}$
 $P_s = 100 \text{ kPa}$
 (b) bearing C
 $W = 3 \text{ kN}$
 $N = 3000 \text{ rpm}$
 $P_s = 100 \text{ kPa}$

□ Bearing A; $T_s = 45^\circ\text{C}$
 ● Bearing B; $T_s = 45^\circ\text{C}$

△ Bearing C; $T_s = 45^\circ\text{C}$
 ▲ Bearing C; $T_s = 35^\circ\text{C}$

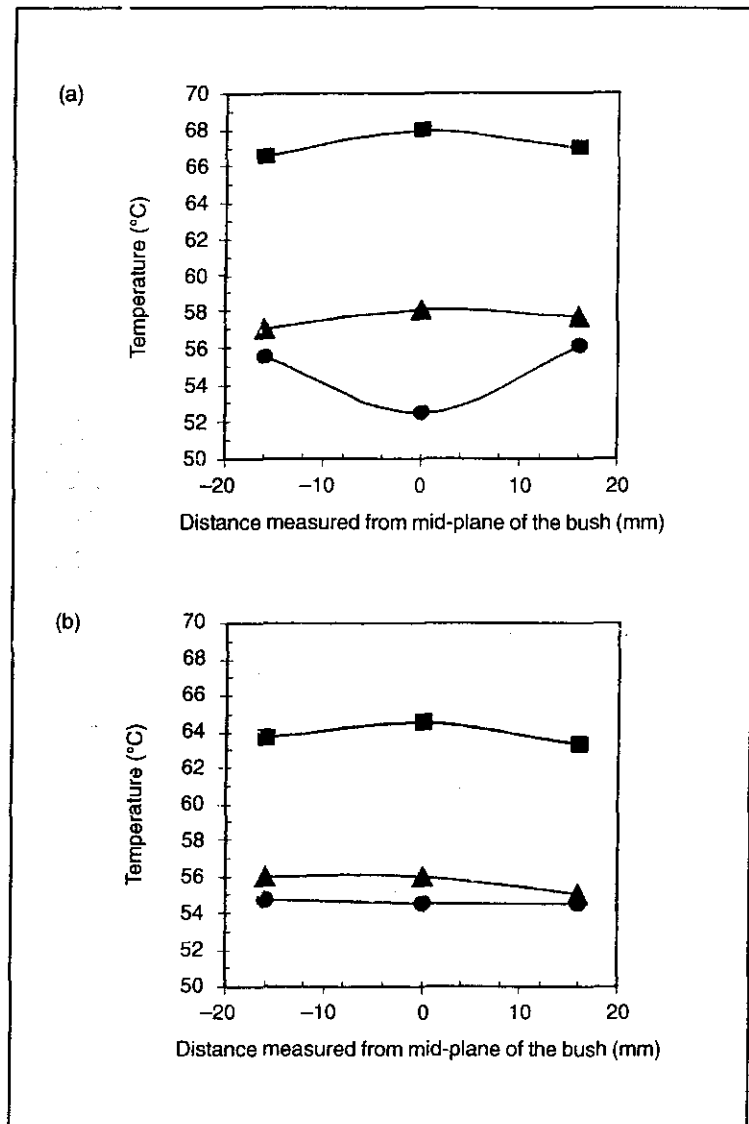


a temperature variation from an initial temperature (23°C) to the average value of the bush inner surface temperature.

The test conditions are listed in **Table 2**. The experimental results for each set of operating conditions were recorded

Figure 5 Axial temperature profiles at the inner surface of the bush for bearings A (a) and B (b), with $W = 4$ kN, $P_s = 100$ kPa, and $N = 4000$ rpm

- $\alpha = 20$ deg
- $\alpha = 150$ deg
- ▲ $\alpha = 340$ deg



after thermal equilibrium had been attained. During testing, the shaft speed was maintained to within ± 2 rpm of the specified value, and the oil supply temperature and oil supply pressure were maintained to within $\pm 1^\circ\text{C}$ and ± 1 kPa of the

specified values, respectively. Each test was performed at least three times on different days and at different times of day. The repeatability of the results was checked. The largest differences observed were $\pm 1.5^\circ\text{C}$ for the maximum bearing temperature, $\pm 4.4\%$ for the flow rate, and $\pm 6.5\%$ for the eccentricity ratio.

RESULTS AND DISCUSSION

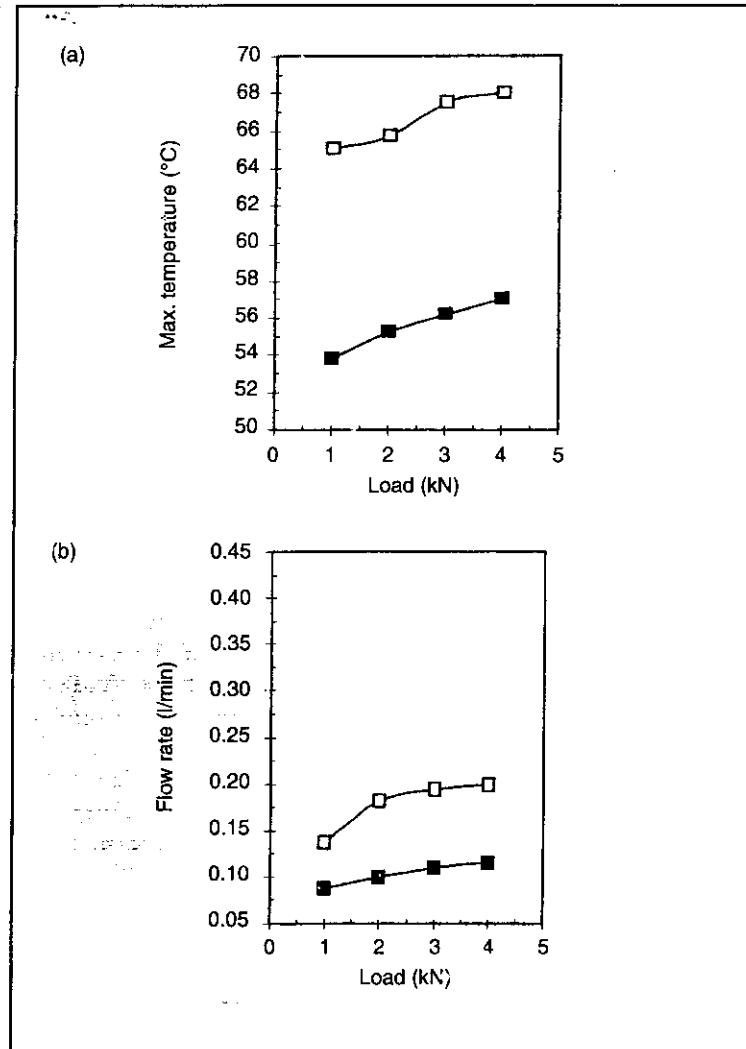
Typical circumferential temperature profiles at the inner surface of the bush are plotted in **Figure 4**. The specific load was 2 mPa for bearings A and B, and 2.4 mPa for bearing C. The maximum bush temperature occurred in a region between 115 and 130° away from the inlet section, as expected in a convergent film region where the rate of shear in the oil is high. The bush temperature in bearing A is considerably higher than in bearing B (**Figure 4(a)**). This is because the radial clearance of bearing A is smaller than that of bearing B, this being a reason for the higher oil shear rate and, consequently, higher heat generation in bearing A. Furthermore, bearing A, having a smaller groove length than bearing B, suffers from a reduction in the cooling effect of the oil supply flow which is lower than in bearing B. **Figure 4(b)** shows the circumferential temperature profiles at the inner surface of bearing C, at two different oil supply temperatures. As might be expected, the higher oil supply temperature results in higher bush temperatures. However, the difference at the maximum temperature (8.6°C) is lower than that at the bearing entry (10°C).

The axial temperature at the inner surface of the bush was carefully examined for all tests carried out with bearings A and B. **Figure 5** shows the axial variation of bush temperature in these bearings under similar operating conditions. The axial temperature gradient was only significant in the vicinity of the groove inlet section of bearing A. In this case, the groove length was significantly smaller than the bush length ($a/b = 0.5$); consequently a significant part of the recirculating flow of hot oil did not mix directly in the groove with the supplied fresh oil. This mixing of oil (oil reformation) took place downstream of the groove, accounting for the temperature variation observed.

The effect of shaft speed on bearing performance characteristics was investigated with bearing A. The experimental results of maximum bush temperature, oil flow rate, and

Figure 6 Measured performance characteristics of bearing A for variable shaft speeds, at fixed $T_s = 45^\circ\text{C}$ and $P_s = 100$ kPa

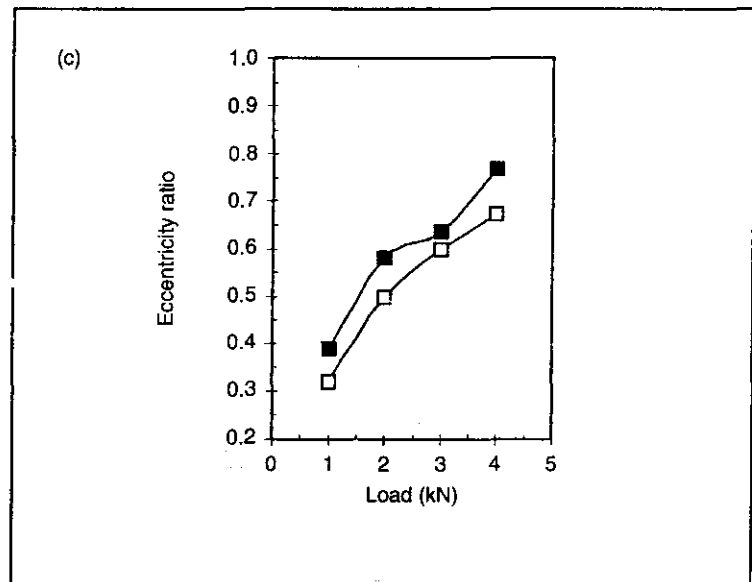
□ $N = 4000$ rpm
 ■ $N = 2000$ rpm



bearing eccentricity ratio are shown in **Figure 6**. It can be observed that the maximum bush temperature and flow rate increased slightly with increasing load. The maximum bearing temperature increased significantly with increasing shaft speed, due to increasing shear rate in the oil. An increase in shaft speed from 2000 to 4000 rpm caused an increase in flow rate of about 48%. The measured eccentricity ratio increased

Figure 6 (continued)
Measured performance characteristics of bearing A for variable shaft speeds, at fixed $T_s = 45^\circ\text{C}$ and $P_s = 100$ kPa

- $N = 4000$ rpm
■ $N = 2000$ rpm



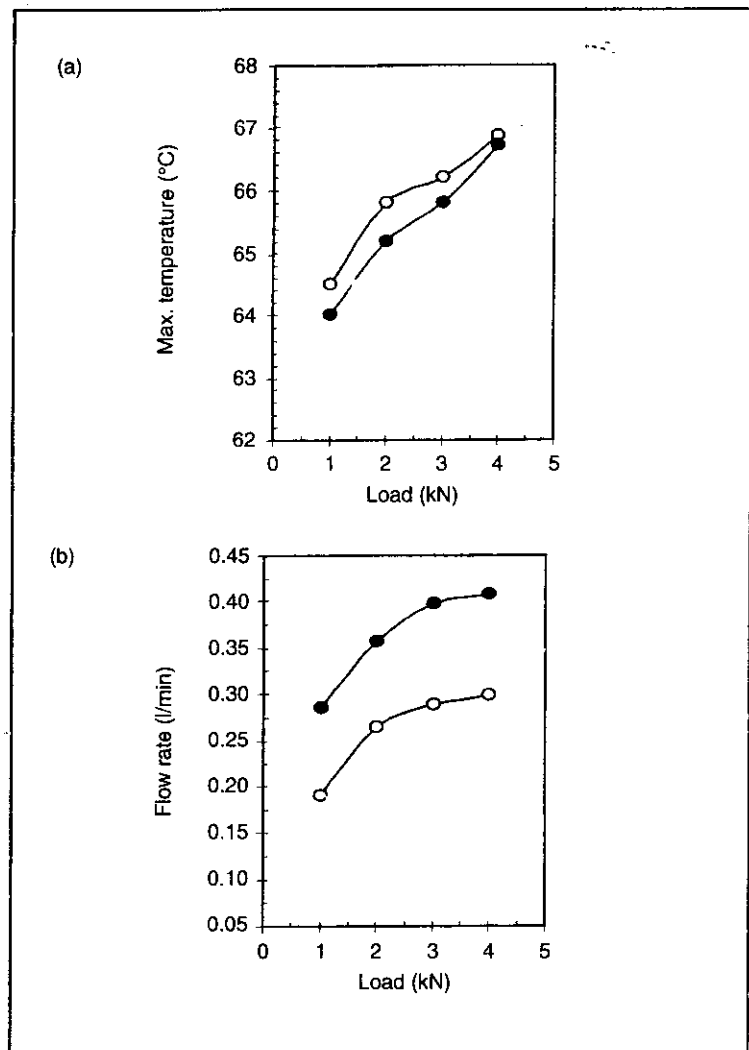
significantly as the load increased. For a shaft speed of 4000 rpm the measured eccentricity ratio was lower than for 2000 rpm. This happens as a result of the prevalence of the hydrodynamic effect over the decrease in oil viscosity induced by higher viscous dissipation.

The performance characteristics of bearing B were measured for two different supply pressures. The results are shown in **Figure 7** (see pp. 158 & 159). It can be observed that there is a significant effect of load on maximum bush temperature. The cooling effect of flow rate, which increases as load increases, was probably offset by the increase in heat generated by viscous dissipation due to an extended full film region. The oil supply pressure did not have a significant effect on the maximum bush temperature. The attitude angle increased with increasing oil supply pressure. This effect was more significant for low applied loads. This may be explained by the existence of a hydrostatic effect of supply pressure over the inlet region, which generates a pressure force component that pushes the shaft, increasing the attitude angle.

A change in oil supply temperature produces changes in the film viscosity field and, as a result, in the film thickness

Figure 7 Measured performance characteristics of bearing B for variable oil supply pressure, at fixed $T_s = 45^\circ\text{C}$ and $N = 4000$ rpm

○ $P_s = 100$ kPa
● $P_s = 300$ kPa

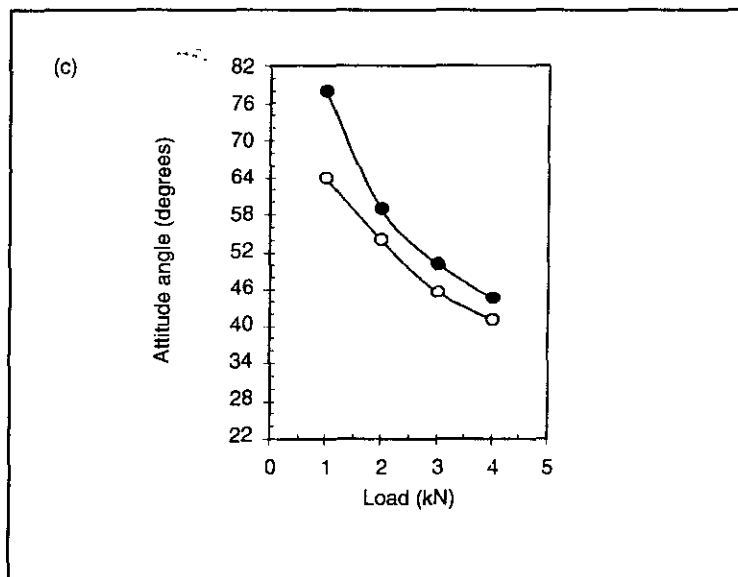


distribution. **Figure 8** (see pp. 160 & 161) shows the measured performance characteristics of bearing C at two different supply temperatures. The decrease in oil supply temperature from 45°C to 35°C led to, on average, decreases of 8°C in the maximum bush temperature and of 19% in the flow rate. Decreasing oil supply temperature will lead to an increase in oil viscosity, resulting in lower flow rates, as was observed.

L. Costa, A.S. Miranda, J.C.P. Claro, and M. Fillon: Temperature, flow, and eccentricity measurements in a journal bearing with a single axial groove at 90° to the load line

Figure 7 (continued)
Measured performance characteristics of bearing B for variable oil supply pressure, at fixed $T_s = 45^\circ\text{C}$ and $N = 4000$ rpm

- $P_s = 100$ kPa
● $P_s = 300$ kPa



Indeed, for fixed applied load and shaft speed, the minimum film thickness increased due to an increase in oil viscosity.

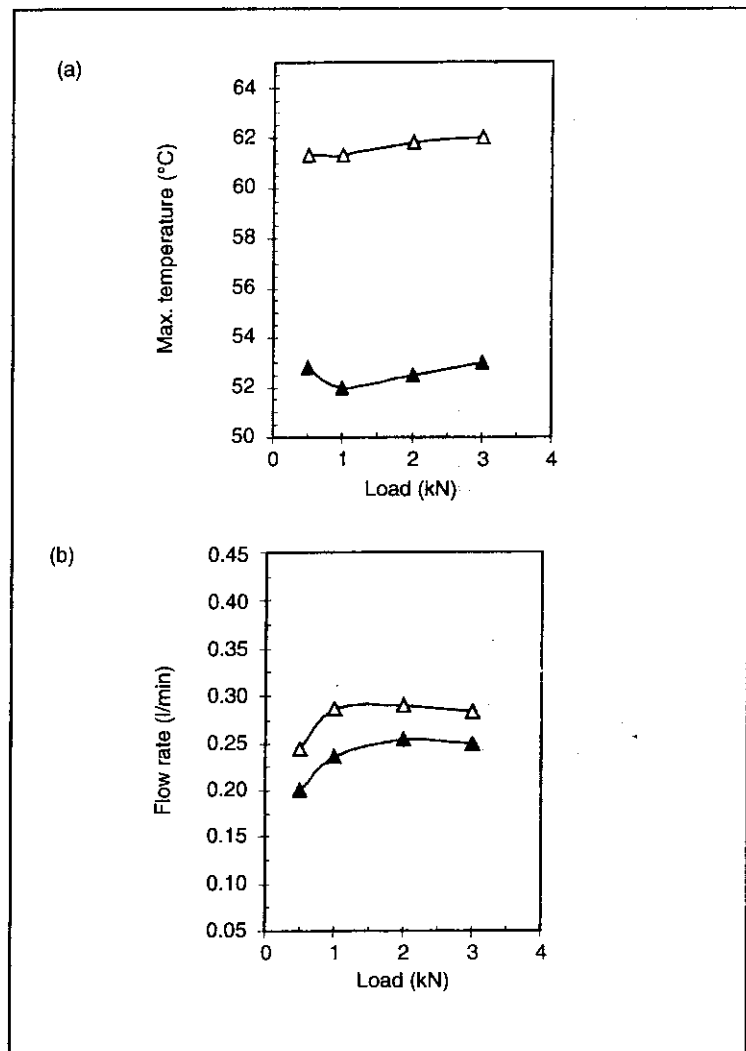
CONCLUSIONS

Laboratory tests have been carried out to investigate the influence of oil supply conditions on bush temperature, oil flow rate, attitude angle, and bearing eccentricity. From the results obtained the following conclusions can be drawn:

- The oil supply temperature has a marked effect on bearing performance. Flow rate and maximum bush temperature increased as the oil supply temperature increased. The opposite occurred for the minimum film thickness.
- The oil supply pressure had a strong influence on oil flow rate, but a small effect on the maximum bush temperature. The influence of the oil supply pressure on attitude angle was significant only for low loads.
- The groove length demonstrated a considerable influence on the axial variation of the bush temperature in the downstream vicinity of the groove, especially at low supply pressures.

Figure 8 Measured performance characteristics of bearing C for variable oil supply temperature, at fixed $P_s = 100$ kPa and $N = 3000$ rpm

▲ $T_s = 35^\circ\text{C}$
 △ $T_s = 45^\circ\text{C}$



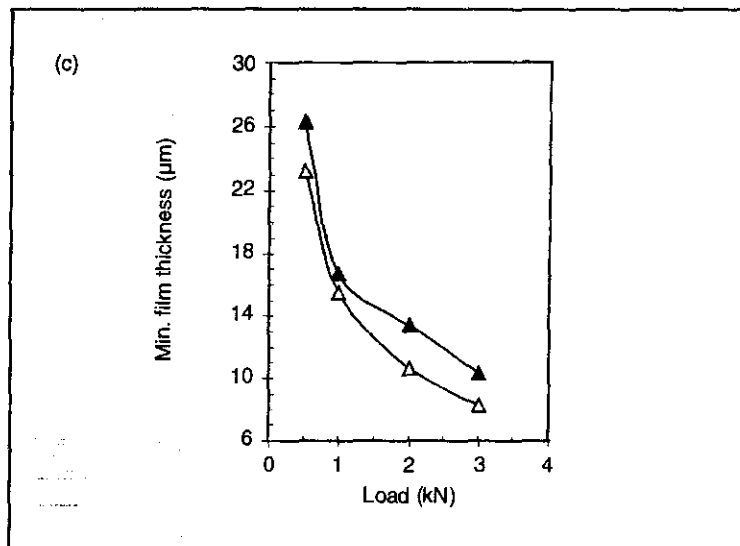
Acknowledgements

The first author is financially supported by the 'Fundação para a Ciência e Tecnologia' (Portugal), through PRAXIS XXI Programme/BD/13922/97. This institution is gratefully acknowledged. The authors would like to thank Petrogal, S.A. (Portugal) for the free supply of the lubricating oil used in the experiments.

L. Costa, A.S. Miranda, J.C.P. Claro, and M. Fillon: Temperature, flow, and eccentricity measurements in a journal bearing with a single axial groove at 90° to the load line

Figure 8 (continued)
Measured performance characteristics of bearing C for variable oil supply temperature, at fixed $P_s = 100$ kPa and $N = 3000$ rpm

▲ $T_s = 35^\circ\text{C}$
△ $T_s = 45^\circ\text{C}$



References

- Fillon, M., Frêne, J., and Boncompain, R., 'Historical aspect and present development on thermal effects in hydrodynamic bearings', *Proc. 13th Leeds-Lyon Symp. Trib.*, Elsevier Tribology Series, 1987, vol. 11, pp. 27-47.
- Swanson, E.E., and Kirk, R.G., 'Survey of experimental data for fixed geometry hydrodynamic journal bearings', *ASME J. Trib.*, **119** (1997) 704-10.
- Hakanson, B., 'The journal bearing considering variable viscosity', *Trans. Chalmers Univ. Technology*, Gothenburg, Sweden, 1965, p. 298.
- Costa, L., Fillon, M., Miranda, A.S., and Claro, J.C.P., 'An experimental investigation of the effect of groove location and supply pressure in the THD performance of a steadily loaded journal bearing', *ASME J. Trib.*, **122** (2000) 227-32.
- Syverud, T., and Tanaka, M., 'Experimental investigation of the effect of shaft heating and cooling on single bore journal bearing', *Wear*, **207** (1997) 112-17.
- Ma, M.T., and Taylor, C.M., 'Effects of oil temperature on the performance of an elliptical bearing', *Proc. 21st Leeds-Lyon Symp. Trib.*, Elsevier Tribology Series, 1995, vol. 30, pp. 43-51.
- Gethin, D.T., and El-Deihi, M.K.I., 'Thermal behaviour of a twin axial groove bearing under varying loading direction', *Proc. IMechE, Part C*, **204** (1990) 77-90.
- Tanaka, M., 'Recent analyses and designs of thick-film bearings', *New Directions in Tribology, First World Tribology Congress*, IMechE, 1997, pp. 411-33.
- Pinkus, O., *Thermal Aspects of Fluid Film Tribology*, ASME Press, 1990.
- Claro, J.C.P., 'Reformulação do Método de Cálculo de Chumaceiras Radiais Hidrodinâmicas, Análise do Desempenho Considerando as Condições de Alimentação', Ph.D. thesis, University of Minho, Portugal, 1994.

This paper was first presented at Nordtrib, Ebeltoft, Denmark.